# On the Bombardment of $Li_2O$ and C by Alpha-Particles and Deuterons*

ISADORE B. BERLMAN**
*Physics Department, Washington University, St. Louis, Missouri*
(Received June 9, 1950)

Photographic nuclear emulsions were used to record the scattered and recoiling particles when $Li_2O$ and C targets were each independently bombarded by 10-Mev deuterons and 20-Mev alpha-particles. The 1.0-Mev level in $C^{13}$ has been confirmed and a new level at 6.8 Mev in $C^{13}$ has been determined. The relative scattering of deuterons and alpha-particles from nuclei in the ground state and in their various nuclear energy levels are illustrated. Finally the alpha-particle range-energy curve, as applied to Ilford E-1 nuclear emulsions, has been modified at higher energies.

## I. INTRODUCTION

THE Washington University cyclotron was used as a source of 10-Mev deuterons, and 20-Mev alpha-particles. These particles were independently made to impinge on a thin $Li_2O$ target or on a thin carbon target. In each case the recoiling and scattered particles were recorded in Ilford E-1 nuclear emulsion plates which were set at predetermined angles to the cyclotron beam. From an analysis of the track lengths certain conclusions were drawn as to energy levels and transmutation products.

## II. APPARATUS

The beam from the cyclotron enters the scattering chamber[1] through a collimator and impinges on a target held in the center of the chamber. A large annular ring contains slits which define the various directions of the scattered particles. Around the periphery of the ring are steel blocks the upper surfaces of which are inclined at 5° to the horizontal. Photographic plates are cut to size and placed on these blocks to detect the scattered and recoiling particles. The undeflected beam enters the collector cup directly opposite the inlet. *O* rings are used to seal various joints in the system so that the experiment can be run under vacuum conditions. The apparatus meets Bethe's[2] requirements for good geometry.

Gold leaf, 0.88 mg/cm$^2$, served as a target backing on which the carbon and the lithium oxide were deposited. The carbon target was prepared by burning camphor and letting the resulting smoke deposit on a target holder. Approximately 0.14 mg/cm$^2$, corresponding to a thickness of $4\times10^{-4}$ cm, was deposited. The energy lost by alpha-particles on penetrating the complete target amounted to 44 kev for the carbon and 50 kev for two layers of gold leaf. For deuterons, the energy loss was approximately one-fourth of this amount.

The lithium-oxide target was prepared by burning metallic lithium in an iron crucible. Traces of carbon impurity were unavoidable. The energy loss of alpha-particles on passing through the lithium-oxide coating

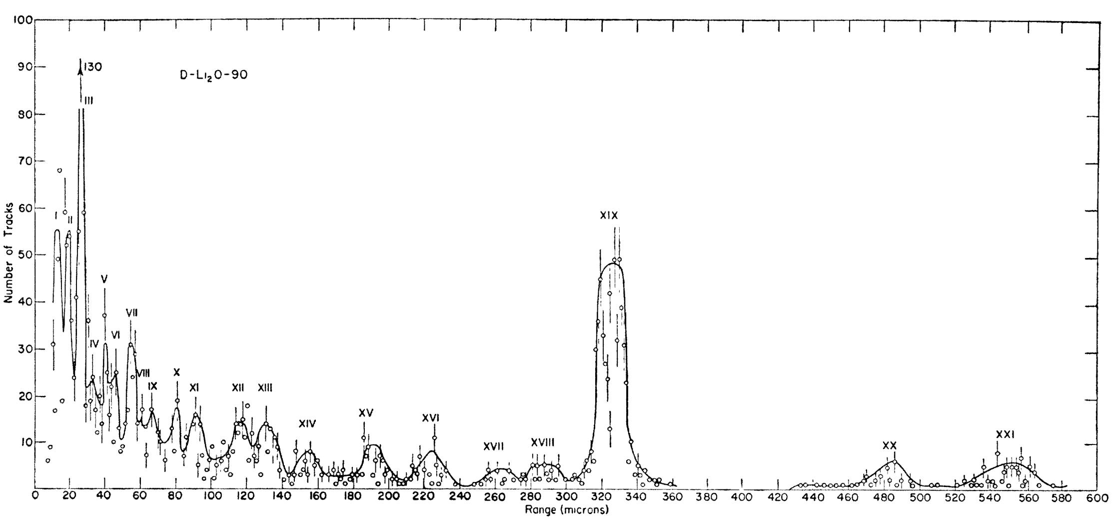


FIG. 1. Distribution in range of particles resulting from the bombardment of $Li_2O$ by deuterons. The angle of recoil is 90° to the cyclotron beam.

* Assisted by the joint program of the ONR and AEC.
** Present Address: Argonne National Laboratory, Chicago, Illinois.
[1] Originally constructed by K. B. Mather, subsequently modified by this author.
[2] M. S. Livingston and H. A. Bethe, Rev. Mod. Phys. 9, 278 (1937).

TABLE I. $D-Li_2O-90$.

| Peak number | Reaction | Level (Mev) | Q (Mev) | E (Mev) | Range (microns) | Observed range (microns) |
|---|---|---|---|---|---|---|
| XXI | $O^{16}(d,p)O^{17}$ | 0 | 1.94 | 10.08 | 565 | 555 |
| | $C^{12}(d,p)C^{13}$ | 0 | 2.7 | 10.3 | 586 | |
| XX | $O^{16}(d,p)O^{17*}$ | 0.88 | 1.06 | 9.25 | 491 | 485 |
| XIX | $Au^{179}(d,d)Au^{179}$ | 0 | 0 | 9.7 | 328 | 326 |
| XVIII | $C^{12}(d,p)C^{13*}$ | 3.95 | −1.25 | 6.64 | 288 | 288 |
| XVII | $Li^7(d,p)Li^8$ | 0 | −0.22 | 6.4 | 270 | 265 |
| XVI | $O^{16}(d,d)O^{16}$ | 0 | 0 | 7.7 | 226 | 224 |
| XV | $C^{12}(d,d)C^{12}$ | 0 | 0 | 7.07 | 196 | 192 |
| XIV | $C^{12}(d,p)C^{13*}$ | 6.0 | −3.3 | 4.73 | 158 | 156 |
| XIII | $Li^7(d,d)Li^7$ | 0 | 0 | 5.5 | 131 | 131 |
| XII | $Li^7(d,d)Li^{7*}$ | 0.477 | −0.477 | 5.13 | 117 | 116 |
| | $Li^6(d,d)Li^6$ | 0 | 0 | 4.95 | 111 | |
| XI | $C^{12}(d,d)C^{12*}$ | 3.1 | −3.1 | 4.4 | 95 | 92 |
| | $Li^6(d,d)He^4$ | 0 | 22.2 | 13.6 | 92 | |
| X | $C^{12}(d,d)C^{12*}$ | 3.58 | −3.58 | 4.0 | 80 | 80 |
| IX | $Li^7(d,\alpha)He^5$ | 0 | 14.3 | 11.24 | 67.5 | 66 |
| VIII | $Li^7(d,t)Li^6$ | 0 | 0.98 | 3.75 | 60 | 60 |
| VII | $C^{12}(d,d)C^{12*}$ | 4.5 | −4.5 | 3.2 | 57 | 55.5 |
| VI | $O^{16}(d,\alpha)N^{14}$ | 0 | 3.06 | 8.98 | 49 | 46 |
| Va | $Li^7(d,He^5)He^4$ | 0 | 14.3 | 8.57 | 40.5 | 40 |
| Vb | $C^{12}(d,p)C^{13*}$ | 8.9 | 6.2 | 2.04 | 41 | |
| IV | $O^{16}(d,d)O^{16*}$ | 6.15 | −6.15 | 2.24 | 34 | 33.5 |
| | $O^{16}(d,\alpha)N^{14*}$ | 2.3 | 0.76 | 7.2 | 35 | |
| III | $O^{16}(d,\alpha)N^{14*}$ | 4.0 | −0.94 | 5.87 | 25.5 | 26 |
| II | $O^{16}(d,\alpha)N^{14*}$ | 5.0 | −1.94 | 5.1 | 21 | 19.5 |
| | $O^{16}(d,d)O^{16*}$ | 7.0 | −7.0 | 1.48 | 18 | |
| | $C^{12}(d,\alpha)B^{10}$ | 0 | −1.44 | 4.6 | 18 | |
| I | $O^{16}(d,\alpha)N^{14*}$ | 6.6 | −3.54 | 3.85 | 14 | 13 |
| | $C^{12}(d,\alpha)B^{10*}$ | 0.71 | −7.15 | 4.07 | 15.3 | |

was 62.5 and 18.5 kev for deuterons. Since these target losses were less than the uncertainty in the cyclotron beam energy they were neglected.

Ilford E-1 nuclear emulsion plates of 200 microns thickness were used. Since thick emulsions have a tendency to peel under prolonged vacuum conditions it was found advisable to daub the edges of each plate with Polystyrene Q Dope. The procedure of development of these plates was similar to that recommended by Wilson and Vanselow.[3] A Spencer microscope of 900× magnification and a Wetzlar microscope of 720× magnification were used to measure the tracks on the processed plates.

## III. METHOD

Figure 1 shows the number of tracks *vs.* range resulting from the bombardment of $Li_2O$ by deuterons. The interpretation of the title, $D-Li_2O-90$, is as follows; the first letter indicates the bombarding particle, the second letter or group of letters indicate the type of target bombarded, and the third set (numbers) indicates the angle at which the scattered and recoil particles were recorded. Thus in the present example $Li_2O$ was bombarded by deuterons and the particles were recorded at 90° to the cyclotron beam.

The following equation[4] may be described as the energy-balance equation for a nuclear reaction.

$$(E_c)^{\frac{1}{2}}=\frac{(m_a m_c E_a)^{\frac{1}{2}}}{m_c+m_d}\cos\theta+\left\{\left[\frac{m_d-m_a}{m_c+m_d}+\frac{m_a m_c}{(m_c+m_d)^2}\cos^2\theta\right]E_a+\frac{m_d Q}{m_c+m_d}\right\}^{\frac{1}{2}}. \quad (1)$$

The subscript $a$ refers to the incident particle, and $c$ and $d$ to the recoil particles. $E_c$ is the energy of the recoil or scattered particle when the energy of the reaction,

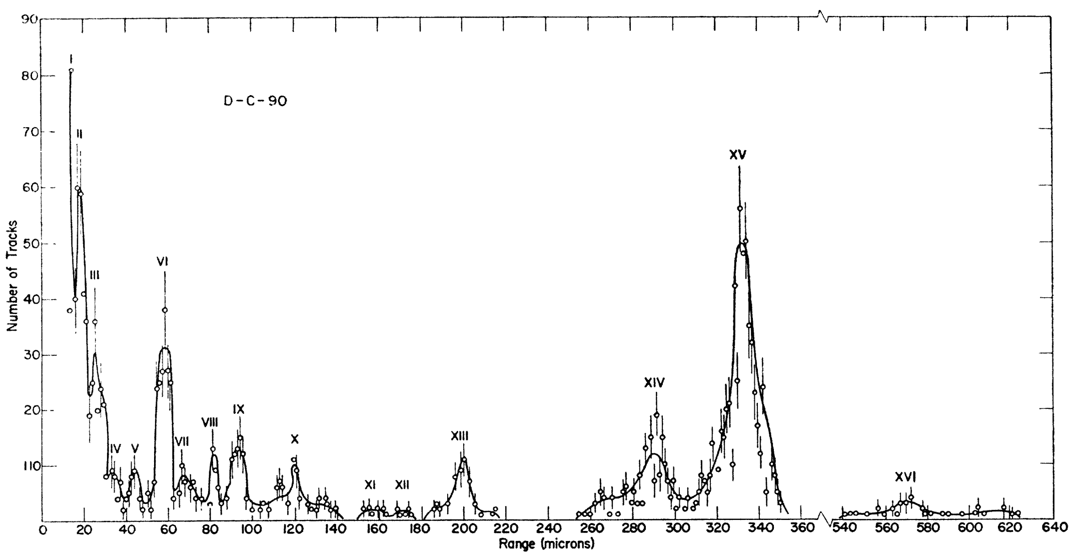


FIG. 2. Distribution in range of particles resulting from the bombardment of a carbon target by deuterons. The angle of recoil is 90° to the cyclotron beam. There are no tracks in the section from 360 to 540 microns. This section was therefore omitted for reasons of space economy.

[3] M. J. Wilson and W. Vanselow, Phys. Rev. **75**, 1144 (1949).
[4] J. Mattauch, *Nuclear Physics Tables* (Interscience Publishers, Inc., New York, 1946), p. 59.

$Q$, the angle of recoil in the laboratory system, $\theta$, and the energy of the incident particle, $E_a$, are known. From the recoil energy and the use of the proper range-energy curve, the range of the particle in the emulsion can be computed.

The problem involved in analyzing an experimental curve showing the number of recoils with any given range, is to determine, largely by a method of trial and error, the nuclear reaction which is responsible for each set of recoils. The choice of the proper reaction is quite tedious at times because of the numerous possibilities. Thus if a 10-Mev deuteron is the bombarding particle, the recorded particle may be a proton, a deuteron, a triton, or an alpha-particle, and any one of these recoil particles may have several recoil energies associated with it depending on the number and prominence of the energy levels in the resultant nucleus. Finally these permutations must be calculated not only for all the known elements in the target but also for the suspected impurities. By the use of Eq. (1) the recoil energy or energies of each possible recoil particle for each possible nuclear reaction are determined for a given angle. This angle is the angle with respect to the cyclotron beam in the laboratory system at which the nuclear plate is set to receive the recoil particles. Finally, the recoil energy must be converted to range by use of the proper

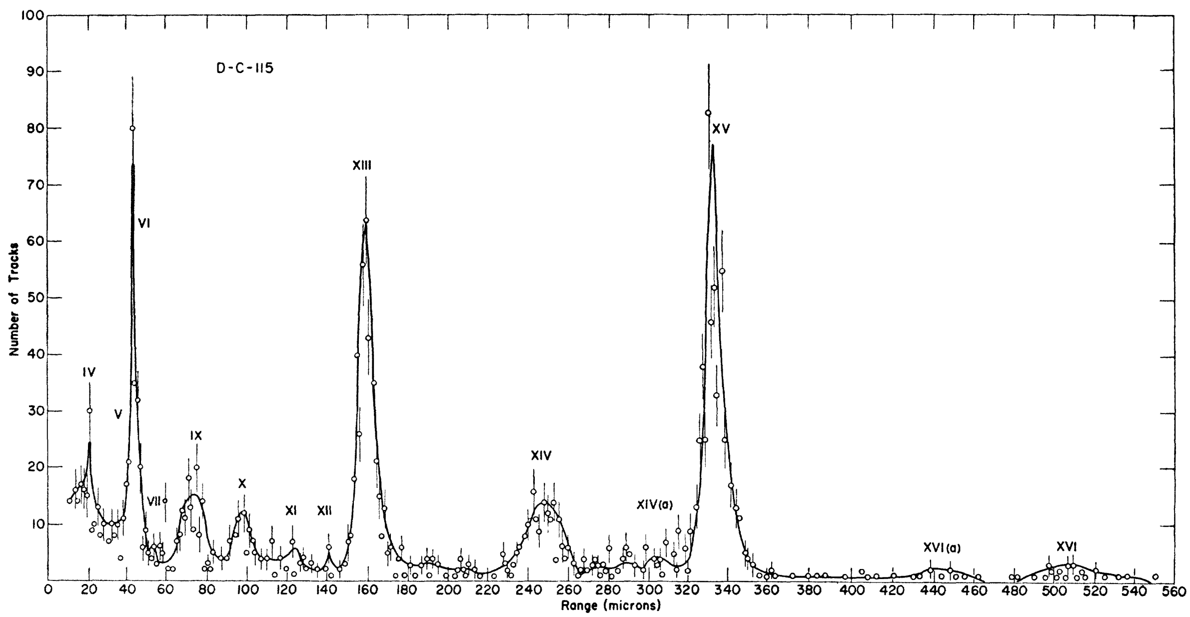


FIG. 3. Distribution in range of particles resulting from the bombardment of a carbon target by deuterons. The angle of recoil is 115° to the cyclotron beam.

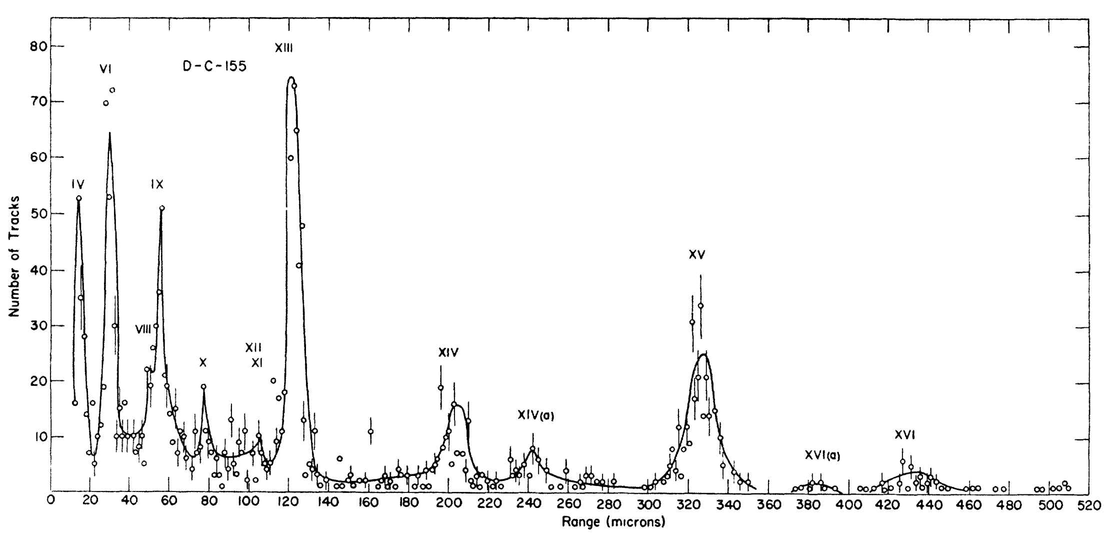


FIG. 4. Distribution in range of particles resulting from the bombardment of a carbon target by deuterons. The angle of recoil is 155° to the cyclotron beam.

TABLE II. $D-C-90$.

| Peak number | Reaction | Level (Mev) | $Q$ (Mev) | $E$ (Mev) | Range (microns) | Observed range (microns) |
|---|---|---|---|---|---|---|
| XVI | $C^{12}(d,p)C^{13}$ | 0 | 2.70 | 10.4 | 591 | 570 |
| XV | $Au^{179}(d,d)Au^{179}$ | 0 | 0 | 9.78 | 332 | 331 |
| XIV | $C^{12}(d,p)C^{13*}$ | 3.95 | −1.25 | 6.68 | 290 | 290 |
| XIII | $C^{12}(d,d)C^{12}$ | 0 | 0 | 7.14 | 200 | 200 |
| XII | $C^{13}(d,t)C^{12}$ | 0 | 1.3 | 7.7 | 176 | 170 |
| XI | $C^{12}(d,p)C^{13*}$ | 6.0 | −3.3 | 4.78 | 160 | 159 |
| X | $C^{12}(d,p)C^{13*}$ | 6.84 | −4.14 | 4.0 | 120 | 120 |
| IX | $C^{12}(d,d)C^{12*}$ | 3.1 | −3.1 | 4.48 | 95 | 92 |
| VIII | $C^{12}(d,d)C^{12*}$ | 3.58 | −3.58 | 4.0 | 80 | 81 |
| VII | $C^{12}(d,p)C^{13*}$ | 8.25 | −5.55 | 2.7 | 64 | 66 |
| VI | $C^{12}(d,d)C^{12*}$ | 4.5 | −4.5 | 3.28 | 59 | 60 |
| | $C^{13}(d,\alpha)B^{11}$ | 0 | 5.12 | 9.76 | 56 | |
| V | $C^{12}(d,p)C^{13*}$ | 8.9 | −6.2 | 2.1 | 44.0 | 43.5 |
| | $C^{13}(d,\alpha)B^{11*}$ | 2.1 | 3.0 | 8.36 | 44 | |
| IV | $C^{13}(d,\alpha)B^{11*}$ | 4.4 | 0.72 | 6.53 | 30 | 33 |
| | $C^{12}(d,d)C^{12*}$ | 5.5 | −5.5 | 2.4 | 37 | |
| III | $C^{13}(d,\alpha)B^{11*}$ | 5.8 | −0.68 | 5.5 | 23.5 | 25 |
| II | $C^{12}(d,\alpha)B^{10}$ | 0 | −1.44 | 4.68 | 18.6 | 18.5 |
| | $C^{12}(d,\alpha)B^{10*}$ | 0.41 | −1.85 | 4.39 | 17 | |
| I | $C^{12}(d,\alpha)B^{10*}$ | 0.71 | −2.15 | 4.13 | 15.5 | |

TABLE III. $D-C-115$.

| Peak number | Reaction | Level (Mev) | $Q$ (Mev) | $E$ (Mev) | Range (microns) | Observed range (microns) |
|---|---|---|---|---|---|---|
| XVI | $C^{12}(d,p)C^{13}$ | 0 | 2.7 | 9.5 | 510 | 508 |
| XVIa | $C^{12}(d,p)C^{13*}$ | 1.0 | 1.7 | 8.6 | 440 | 442 |
| XV | $Au^{179}(d,d)Au^{179}$ | 0 | 0 | 9.7 | 329 | 330 |
| XIVa | $C^{12}(d,p)C^{13*}$ | 3.1 | −0.4 | 6.77 | 300 | 304 |
| XIV | $C^{12}(d,p)C^{13*}$ | 3.95 | −1.25 | 6.0 | 240 | 246 |
| XIII | $C^{12}(d,d)C^{12}$ | 0 | 0 | 6.2 | 158 | 158 |
| XII | $C^{13}(d,t)C^{12}$ | 0 | 1.31 | 6.55 | 138 | 141 |
| XI | $C^{12}(d,p)C^{13*}$ | 6.0 | −3.3 | 4.2 | 131 | 124 |
| X | $C^{12}(d,p)C^{13*}$ | 6.84 | −4.14 | 3.5 | 97 | 98 |
| IX | $C^{12}(d,d)C^{12*}$ | 3.1 | −3.1 | 3.71 | 72 | 73 |
| VIII | $C^{12}(d,d)C^{12*}$ | 3.58 | −3.58 | 3.4 | 62 | |
| VII | $C^{12}(d,p)C^{13*}$ | 8.25 | −5.55 | 2.26 | 48.5 | 53 |
| VI | $C^{12}(d,d)C^{12*}$ | 4.5 | −4.5 | 2.7 | 44 | |
| | $C^{13}(d,\alpha)B^{11}$ | 0 | 5.12 | 8.35 | 44 | |
| V | $C^{12}(d,p)C^{13*}$ | 8.9 | −6.25 | 1.75 | 32 | not observed |
| | $C^{13}(d,\alpha)B^{11*}$ | 2.1 | 3.0 | 6.38 | 26 | |
| IV | $C^{13}(d,\alpha)B^{11*}$ | 4.4 | 0.72 | 5.32 | 22 | 20 |
| | $C^{12}(d,d)C^{12*}$ | 5.5 | −5.5 | 1.9 | 26 | |

range-energy curve. It then becomes possible to compare the predicted ranges arising from these reactions with the actual peaks observed in the experimental curves. This has been done and Table I shows the correlation of each observed peak in Fig. 1 with the assumed reaction or reactions causing it.

An examination of the experimental curves of number of tracks *vs.* track length shows that while some peaks are sharp and distinct, others are so low as to be scarcely distinguishable from the background. In connection with the low peaks, two comments are made. First, when scattering experiments were conducted using the gold foil alone, a careful examination of the plates showed practically no tracks at all having lengths that did not correspond to scattering from the gold. This absence of "accidentals" or "background" under the same conditions used in regular scattering runs lends assurance to the significance of peaks having only 8 or 10 tracks. While 8 or 10 tracks do not constitute good statistical data, their importance grows when it is known that no tracks at all are the normal expectancy.

The second point concerning the low peaks is that some of them have frankly been located on the basis of known energy levels, where the small number of counts in the present work left the exact location uncertain. This has been done for the purpose of exhibiting the relative heights of the various peaks observed.

The use of Ilford E-1 nuclear emulsions allows one to distinguish clearly between an alpha-particle track and a proton track. The same cannot be said for short proton and deuteron tracks.

Table I correlates each peak of Fig. 1 with the assumed reaction causing it. Thus peak number XXI in Fig. 1 is due to protons from the reactions $O^{16}(d,p)O^{17}$ and $C^{12}(d,p)C^{13}$, see Table I, column two. Column three of this table is marked *level* and indicates that for this peak no energy level is involved and that $O^{17}$ was left

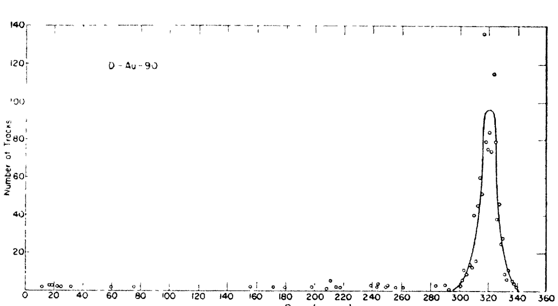


FIG. 5. Distribution in range of particles resulting from the bombardment of a gold target by deuterons. The angle of recoil is 90° to the cyclotron beam.

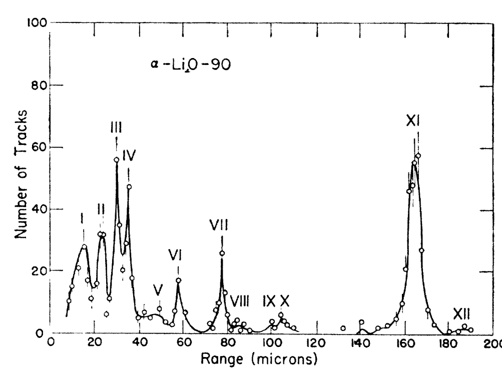


FIG. 6. Distribution in range of particles resulting from the bombardment of a $Li_2O$ target by alpha-particles. The angle of recoil is 90° to the cyclotron beam.

TABLE IV. $D$—C—155.

| Peak number | Reaction | Level (Mev) | $Q$ (Mev) | $E$ (Mev) | Range (microns) | Observed range (microns) |
|---|---|---|---|---|---|---|
| XVI | $C^{12}(d,p)C^{13}$ | 0 | 2.7 | 8.7 | 447 | 450 |
| | $O^{16}(d,p)O^{17}$ | 0 | 1.9 | 8.78 | 450 | |
| XVIa | $C^{12}(d,p)C^{13*}$ | 1.0 | 1.7 | 7.85 | 380 | 382 |
| XV | $Au^{179}(d,d)Au^{179}$ | 0 | 0 | 9.6 | 323 | 328 |
| XIVa | $C^{12}(d,p)C^{13*}$ | 3.1 | −0.4 | 6.07 | 238 | 241 |
| XIV | $C^{12}(d,p)C^{13}$ | 3.95 | −1.25 | 5.35 | 194 | 202 |
| XIII | $C^{12}(d,d)C^{12}$ | 0 | 0 | 5.3 | 124 | 121 |
| XII | $C^{13}(d,t)C^{12}$ | 0 | 1.31 | 5.51 | 105 | 105 |
| XI | $C^{12}(d,p)C^{13*}$ | 6.0 | −3.3 | 3.69 | 105 | 105 |
| X | $C^{12}(d,p)C^{13*}$ | 6.84 | −4.14 | 3.04 | 76 | 77 |
| IX | $C^{12}(d,d)C^{12*}$ | 3.1 | −3.1 | 3.1 | 55 | 56 |
| VIII | $C^{12}(d,d)C^{12*}$ | 3.58 | −3.58 | 2.7 | 45 | 49 |
| VII | $C^{12}(d,p)C^{13*}$ | 8.25 | −5.55 | 1.9 | 37 | |
| VI | $C^{12}(d,d)C^{12*}$ | 4.5 | −4.5 | 2.1 | 31 | 29 |
| | $C^{13}(d,\alpha)B^{11}$ | 0 | 5.12 | 6.9 | 33 | |
| V | $C^{12}(d,p)C^{13*}$ | 8.9 | −6.25 | 1.42 | 24 | |
| | $C^{13}(d,\alpha)B^{11*}$ | 2.1 | 3.02 | 5.7 | 24.5 | |

TABLE V. $\alpha$—$Li_2O$—90.

| Peak number | Reaction | Level (Mev) | $Q$ (Mev) | $E$ (Mev) | Range (microns) | Observed range (microns) |
|---|---|---|---|---|---|---|
| XII | $Li^6(\alpha,d)Be^8$ | 0 | −1.6 | 6.7 | 180.0 | 186 |
| XI | $Au^{179}(\alpha,\alpha)Au^{179}$ | 0 | 0 | 19.6 | 168.0 | 164 |
| X | $Li^7(\alpha,p)Be^{10*}$ | 3.36 | −5.94 | 3.69 | 106.0 | 104 |
| II | $Li^7(\alpha,t)Be^8$ | 0 | −2.56 | 5.42 | 102.0 | 100 |
| VIII | $Li^6(\alpha,d)Be^{8*}$ | 3.1 | −4.7 | 4.2 | 86.0 | 84.5 |
| VII | $O^{16}(\alpha,\alpha)O^{16}$ | 0 | 0 | 12.0 | 78.0 | 77.5 |
| VI | $C^{12}(\alpha,\alpha)C^{12}$ | 0 | 0 | 10 | 0.58 | 57.5 |
| | $Li^7(\alpha,d)Be^9$ | 0 | −7.1 | 3.38 | 61.0 | |
| V | $Li^7(\alpha,t)Be^{8*}$ | 3.1 | −5.66 | 3.16 | 48.0 | 49 |
| | $Li^6(\alpha,d)Be^{8*}$ | 4.8 | −6.4 | 2.86 | 56.0 | |
| IV | $O^{16}(\alpha,\alpha)O^{16*}$ | 6.0 | −6.0 | 7.2 | 35.0 | 35 |
| | $O^{16}(\alpha,\alpha)O^{16*}$ | 6.15 | −6.15 | 7.1 | 34.0 | |
| III | $O^{16}(\alpha,\alpha)O^{16*}$ | 7.0 | −7.0 | 6.75 | 32.0 | 29.5 |
| | $C^{12}(\alpha,\alpha)C^{12*}$ | 4.5 | −4.5 | 6.6 | 30.5 | |
| II | $Li^7(\alpha,\alpha)Li^7$ | 0 | 0 | 5.46 | 23 | |
| | $Li^7(\alpha,\alpha)Li^{7*}$ | 0.477 | −0.477 | 5.16 | 21.5 | |
| I | $Li^6(\alpha,\alpha)Li^6$ | 0 | 0 | 4.0 | 15.0 | 15.5 |

in the ground state. The energy of reaction, $Q$, is given in column four as 1.94 Mev. $Q$ is usually obtained either from Lauritsen[5] or, if not given there, is computed from the masses involved.[6,7] Column five gives the recoil energy, $E$, of the light particle as 10.08 Mev. This value is obtained from Eq. (1) assuming that the bombarding energy of the deuteron is 9.9 Mev. The range is computed from the range-energy curve for protons and appears in column six. The observed range appears in column seven.

## IV. RESULTS

(a) Reactions caused by 9.9-Mev deuteron bombardment of a thin $Li_2O$ target. See Fig. 1.

1. $O^{16}(d,p)O^{17}$

| Peak | Energy levels in $O^{17}$ | Comments |
|---|---|---|
| XXI | Ground state | XXI and XX may contain some protons from $C^{12}(d,p)C^{13}$ (from carbon contaminant). |
| XX | 0.88 Mev | |

2. $O^{16}(d,d)O^{16}$

| Peak | Energy levels in $O^{16}$ | Comments |
|---|---|---|
| XVI | Ground state | Evidence for an $O^{16}$ level at 6.0 Mev as listed by Lauritsen[5] is obscured by the background of tracks. |
| IV | 6.15 Mev | |
| II | 7.0 Mev | |

3. $O^{16}(d,\alpha)N^{14}$

| Peak | Energy levels in $N^{14}$ | Comments |
|---|---|---|
| VI | Ground state | II and I are somewhat obscured by alpha-particles from $C^{12}(d,\alpha)B^{10}$. Evidence for $N^{14}$ levels at 5.5 or 6.1 Mev as listed by Lauritsen[5] is obscured by the background tracks. |
| IV | 2.3 Mev | |
| III | 4.0 Mev | |
| II | 5.0 Mev | |
| I | 6.6 Mev | |

[5] T. Lauritsen, Preliminary Report No. 5, National Research Council, Nuclear Science Series (1949).
[6] *Handbook of Chemistry and Physics* (1949), thirty-first edition.
[7] K. T. Bainbridge, Preliminary Report No. 1, National Research Council, Nuclear Science Series (1948).

4. $C^{12}(d,p)C^{13}$

| Peak | Energy levels in $C^{13}$ | Comments |
|---|---|---|
| XXI | Ground state | No evidence for levels in $C^{13}$ at 5.0 and 8.25 Mev as listed by Lauritsen.[5] |
| XVIII | 3.95 Mev | |
| XIV | 6.0 Mev | |
| V | 8.9 Mev | |

5. $C^{12}(d,d)C^{12}$

| Peak | Energy levels in $C^{12}$ | Comments |
|---|---|---|
| XV | Ground state | See below. |
| XI | 3.1 Mev | |
| X | 3.58 Mev | |
| VII | 4.5 Mev | |

Further discussion of this section will be found in paragraph (b).

6. $Li^7(d,p)Li^8$

| Peak | Energy levels in $Li^8$ | Comments |
|---|---|---|
| XVII | Ground state | Further decay of $Li^8$ is not considered since the half-life is relatively long in comparison to the collision process. |

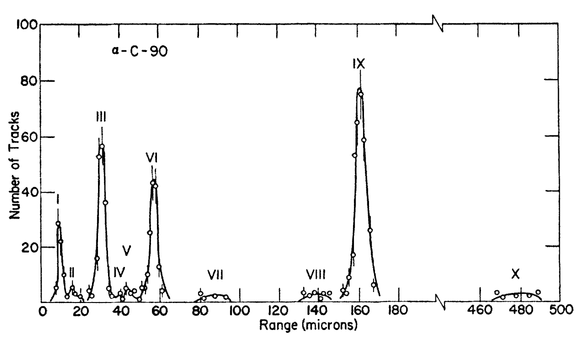


FIG. 7. Distribution in range of particles resulting from the bombardment of a carbon target by alpha-particles. The angle of recoil is 90° to the cyclotron beam.

TABLE VI. $\alpha-C-90$.

| Peak number | Reaction | Level (Mev) | Q (Mev) | E (Mev) | Range (microns) | Observed range (microns) |
|---|---|---|---|---|---|---|
| X | $C^{12}(\alpha,p)N^{15}$ | 0 | −4.92 | 9.14 | 480 | 480 |
| IX | $Au^{179}(\alpha,\alpha)Au^{179}$ | 0 | 0 | 19.13 | 161.5 | 161 |
| VIII | $C^{12}(\alpha,p)N^{15*}$ | 5.4 | −10.12 | 4.26 | 134 | 138 |
| VII | $C^{12}(\alpha,p)N^{15*}$ | 6.2 | 11.1 | 3.33 | 90 | 85 |
| VI | $C^{12}(\alpha,\alpha)C^{12}$ | 0 | 0 | 10 | 58 | 58 |
| V | $C^{12}(\alpha,p)N^{15*}$ | 7.5 | 12.4 | 2.1 | 43.5 | 44 |
| IV | $C^{12}(\alpha,\alpha)C^{12*}$ | 3.1 | −3.1 | 7.68 | 39 | 39 |
| III | $C^{12}(\alpha,\alpha)C^{12*}$ | 4.5 | −4.5 | 6.7 | 31 | 30 |
| II | $C^{12}(\alpha,\alpha)C^{12*}$ | 7.3 | −7.3 | 4.5 | 18 | 15.5 |
| I | $C^{12}(\alpha,\alpha)C^{12*}$ | 9.5 | −9.5 | 2.88 | 10 | 8.5 |

7. $Li^7(d,d)Li^7$

| Peak | Energy levels in $Li^7$ | Comments |
|---|---|---|
| XIII | Ground state | Elastically scattered deuterons from $Li^6$ will also contribute to XII. |
| XII | 0.48 Mev | |

The number of observed tracks was too small to permit any conclusions about additional excited states in $Li^7$ in the region from 0.5 Mev to 1 Mev.

8. $Li^7(d,\alpha)He^5$

By using the corrected range-energy curve the $Q$ of this reaction is 14.3 Mev as given by Lauritsen.[5]

(b) Reactions caused by 10-Mev deuteron bombardment of a thin C target. See Figs. 2 to 4, also Tables II to IV.

1. $C^{12}(d,p)C^{13}$

| Peak | Energy levels in $C^{13}$ | Comments |
|---|---|---|
| XVI | Ground state | XVIa does not appear at 90° to the cyclotron beam. X is a new level in $C^{13}$ that appears with about the same intensity as XIVa does. |
| XVIa | 1.0 Mev | |
| XIVa | 3.1 Mev | |
| XIV | 3.95 Mev | |
| XI | 6.0 Mev | |
| X | 6.84 Mev | |
| VII | 8.25 Mev | |
| V | 8.9 Mev | |

It is of interest to compare the relative intensities of these peaks and how they change as one goes to larger angles as shown in the successive figures.

2. $C^{12}(d,d)C^{12}$

| Peak | Energy levels in $C^{12}$ | Comments |
|---|---|---|
| XIII | Ground state | The VIII is somewhat doubtful as it appears only at 90° and not at 115° and 155°. VI and IV contain some alpha-particles from the reaction $C^{13}(d,\alpha)B^{11}$. There is 1.1 percent $C^{13}$ in the target. |
| IX | 3.1 Mev | |
| VIII | 3.85 Mev | |
| VI | 4.5 Mev | |
| IV | 5.5 Mev | |

3. $C^{13}(d,\alpha)B^{11}$

| Peak | Energy levels in $B^{11}$ | Comments |
|---|---|---|
| VI | Ground state | Since there is so little $C^{13}$ in the target it is doubtful whether this reaction contributes appreciably to the observed peaks. |
| V | 2.1 Mev | |
| IV | 4.4 Mev | |
| III | 5.8 Mev | |

4. $C^{12}(d,\alpha)B^{10}$

| Peak | Energy levels in $B^{10}$ | Comments |
|---|---|---|
| II | 0 and 0.41 Mev | The ground state and the 0.41-Mev level fall close enough together to be represented by one peak, II. |
| I | 0.71 Mev | |

(c) Figure 5 is a background run to demonstrate that there is only one peak resulting from the bombardment of gold by deuterons, and that it is due to elastically scattered deuterons.

(d) Reactions caused by 20-Mev alpha-particle bombardment of a thin $Li_2O$ target. See Fig. 6 and Table V.

1. $O^{16}(\alpha,\alpha)O^{16}$

| Peak | Energy levels in $O^{16}$ | Comments |
|---|---|---|
| VII | Ground state | The 0.88-Mev level does not appear. The resolution of the instrument does not allow for the separation of the 6.0- and 6.15-Mev levels. III contains some alpha-particles elastically scattered from carbon. |
| IV | 6.0 and 6.15 Mev | |
| III | 7.0 Mev | |

2. $C^{12}(\alpha,\alpha)C^{12}$

| Peak | Energy levels in $C^{12}$ | Comments |
|---|---|---|
| VI | Ground state | That VI and III are correctly identified is readily shown by superimposing Fig. 7 on Fig. 6. |
| III | 4.5 Mev | |

3. $Li^7(\alpha,p)Be^{10}$

| Peak | Energy levels in $Be^{10}$ | Comments |
|---|---|---|
| X | 3.36 Mev | There are a few tracks from the ground level but too few to be shown by a peak. These tracks are easily recognized since they are produced by singly charged particles. |

4. $Li^7(\alpha,d)Be^9$

| Peak | Energy levels in $Be^9$ | Comments |
|---|---|---|
| VI | Ground state | |

5. $Li^7(\alpha,t)Be^8$

| Peak | Energy levels in $Be^8$ | Comments |
|---|---|---|
| IX | Ground state | In V there are probably a few deuterons due to the reaction $Li^6(\alpha,d)Be^{8*}$ where $Be^{8*}$ is in the 4.8-Mev level. The further decay of $Be^8$ into two alpha-particles is not considered since no broad peak as would result from such a three-body process has been observed. |
| V | 3.1 Mev | |

6. $Li^7(\alpha,\alpha)Li^7$

| Peak | Energy levels in $Li^7$ | Comments |
|---|---|---|
| II | Ground state and 0.48-Mev level | The instrument is incapable of distinguishing between these two states at low energies. |

7. $Li^6(\alpha,\alpha)Li^6$

| Peak | Energy levels in $Li^6$ | Comments |
|---|---|---|
| I | Ground state | To obtain greater recoil energies a smaller scattering angle will be necessary. |

(e) Reactions caused by 20-Mev alpha-particle bombardment of a thin carbon target. See Fig. 7 and Table VI.

1. $C^{12}(\alpha,p)N^{15}$

| Peak | Energy levels in $N^{15}$ | Comments |
|---|---|---|
| X | Ground state | |
| VIII | 5.4 Mev | |
| VII | 6.2 Mev | |
| V | 7.5 Mev | |

2. $C^{12}(\alpha,\alpha)C^{12}$

| Peak | Energy levels of $C^{12}$ | Comments |
|---|---|---|
| VI | Ground state | If IV exists, it is a very weak peak. Lauritsen[5] lists IV as a doubtful level. Other doubtful levels at 3.58 and 5.5 Mev do not appear. |
| IV | 3.1 Mev | |
| III | 4.5 Mev | |
| II | 7.3 Mev | |
| I | 9.5 Mev | |

From peak XI in Fig. 6 and IX in Fig. 7, which are due to the elastic scattering of alpha-particles from gold, it was found necessary to modify the range-energy curve of Lattes[8] at higher energies. Other evidence as to a need for modification came from an alpha-alpha-bombardment when the recoiling and scattered particles were recorded at small angles. The observed ranges fell short of the predicted ranges when Lattes' curve was used. This was true for the three aforementioned cases even after all possible corrections were made. If the beam energy were lower than 20 Mev, i.e., 17.5 Mev, then XI in Fig. 6 and IX in Fig. 7 would be correctly identified but then the other peaks in Figs. 6 and 7 would be displaced too far to the right. Therefore it was assumed that the bombarding energy was 20 Mev, that the lower portion of the alpha-energy range curve, below 10 Mev, was correct, but that above 10 Mev a modification was necessary. This modification was made from the proton range-energy curve by assuming that an alpha-particle and a proton of the same velocity have the same range. The corrected curve has already been published.

[8] Lattes, Fowler, and Cuer, Proc. Phys. Soc. London **59**, 883 (1947).

## V. CONCLUSION

The 1.0-Mev level in $C^{13}$ has been confirmed, and a new level at 6.8 Mev has been determined. The proton group giving rise to the 1.0-Mev level is small statistically, consisting of only approximately 11 tracks at 115°, yet this number is large compared to the expected background at this range and is an appreciable fraction of the 33 proton tracks observed which resulted from $C^{13}$ in the ground state. A level in $C^{12}$ at 3.58 Mev has been found at 90° but the results are doubtful because of non-appearance at 115° and 155° or under alpha-particle bombardment. The relative scattering of deuterons and alpha-particles from nuclei in the ground state and in the various nuclear energy levels are illustrated. The results indicate that 10-Mev deuterons are more effective in studying energy levels than are 20-Mev alpha-particles. Finally the alpha-particle range-energy curve, as applied to Ilford E-1 nuclear emulsions, has been modified at higher energies for alpha-particles.

This author wishes to thank Messrs. Chia-Hua Chang and Wen-Jsao Yang for their careful reading of the plates, and Dr. Robert N. Varney for his constructive criticism.

PHYSICAL REVIEW VOLUME 80, NUMBER 5 DECEMBER 1, 1950

# The New Element Berkelium (Atomic Number 97)*

S. G. Thompson, A. Ghiorso, and G. T. Seaborg
*Radiation Laboratory and Department of Chemistry, University of California, Berkeley, California*

(Received July 24, 1950)

An isotope of the element with atomic number 97 has been discovered as a product of the helium ion bombardment of americium. This isotope decays with the emission of alpha-particles of maximum energy 6.72 Mev (30 percent) and it emits lower energy alpha-particles of energies 6.55 Mev (53 percent) and 6.20 Mev (17 percent). The half-life of this isotope is 4.6±0.2 hr. and it decays primarily by electron capture with about 0.1 percent branching decay by alpha-particle emission. The mass number is probably 243 as indicated by chemical separation of the alpha-particle and electron-capture daughters. The name berkelium, symbol Bk, is proposed for element 97.

The chemical separation of element 97 from the target material and other reaction products was made by combinations of precipitation and ion exchange adsorption methods making use of its anticipated (III) and (IV) oxidation states and its position as a member of the actinide transition series. The distinctive chemical properties made use of in its separation and the equally distinctive decay properties of the particular isotope constitute the principal evidence for the new element.

The isotope $Cm^{243}$ is identified experimentally as a result of its production as a decay product of $Bk^{243}$. The $Cm^{243}$ decays by the emission of alpha-particles of maximum energy 5.89 Mev (15 percent) and lower energy alpha-particles of energy 5.79 Mev (85 percent); the half-life for alpha-particle emission is estimated to be roughly 100 yr.

## I. INTRODUCTION

THE transuranium elements numbers 96, curium, and 95, americium, were discovered in 1944, the first by Seaborg, James, and Ghiorso,[1] the second by Seaborg, James, and Morgan.[2] The search for transcurium elements was begun by us in the fall of 1945. It was anticipated[3] that element 97 as eka-terbium in the actinide transition series would possess oxidation states (III) and (IV) with properties similar to curium in the (III) oxidation state and to plutonium (IV) in

* This work was performed under the auspices of the AEC.

[1] Seaborg, James, and Ghiorso, *The Transuranium Elements: Research Papers* (McGraw-Hill Book Company, Inc., New York, 1949), Paper No. 22.2, National Nuclear Energy Series, Plutonium Project Record, Vol. 14B.

[2] Seaborg, James, and Morgan, National Nuclear Energy Series, see reference 1, Paper No. 22.1.

[3] G. T. Seaborg, Nucleonics **5**, No. 5, 16 (1949).